Impacts of increasing low-level shear on supercells during the evening transition

Brice E. Coffer* and Matthew D. Parker

Department of Marine, Earth, and Atmospheric Sciences, North Carolina State University, Raleigh, NC

1. Introduction

A commonly observed characteristic of severe weather events in the central United States is an increase in shear in the lowest one kilometer during the late afternoon and early evening hours (Maddox 1993). Decoupling of the surface layer with the rest of the planetary boundary layer during the early evening transition (EET) causes a decrease in the surface wind speed (Nieuwsadt 1985) and the development of a nocturnal low-level jet (LLJ; van de Wiel et al. 2010). A defining characteristic of the LLJ is a veering of the wind vector with time and the development of a supergeostrophic wind maximum.

The United States Great Plains exhibits a distinct maximum in the climatology of LLJs (e.g. Bonner 1968). LLJs have been studied extensively due to their widespread impacts, including moisture transport, nocturnal rain maxima, transportation of pollutants, dust storms, wildfires, and strong vertical wind shear. Research on the latter has mainly focused on aviation hazards and wind energy, however the evening evolution of the boundary layer wind profile could have profound impacts on severe convective storms, as well as tornadoes.

The second Verification of the Origins of Rotation in Tornadoes Experiments (VORTEX2; Wurman et al. 2012) collected unprecedented observations of numerous supercells. One mission of this campaign was to understand the spatial and temporal variability in the environmental of supercells through numerous near-storm soundings (Parker 2013; P13). When comparing the early-in-life versus late-in-life composite soundings, P13 found that, although the 0-6km shear vector magnitude remained identical, over time, the winds below 2-3 km above ground layer (AGL) increase in speed. This results in dramatic increases in low-level environmental storm-relative helicity (SRH) and bulk shear. Storm chasers often refer anecdotally to the phenomenon of "six-o'clock magic", because supercells seem to have the propensity to produce tornadoes in the early evening hours, as the sun sets. Indeed, the tornado climatology of the United States shows a maximum frequency of tornadoes during this time frame, especially in the Great Plains[1]. This is likely due to lower lifted condensation levels (LCL) and higher SRH.

It is unclear how storms directly respond to the changes in shear during the EET, nor how changes in shear interplay with changes in stability. We hypothesize that the evolving low-level shear leads to changes in the storm's profile of vertical vorticity and/or changes in the low-level dynamic lifting of air. This could be important for tornadogenesis, for example, in highly idealized, toy model simulations, Markowski and Richardson (2013) have shown that surface vortices strengthen when the storm's outflow temperature is not exceedingly cold and the dynamic low-level lifting of outflow air is large.

The purpose of this paper is to investigate the impacts increasing low-level environmental shear upon mature supercells in full-physics supercell simulations using observational data obtained from the VORTEX2 field campaign. Details regarding the methods are described in Section 2. Results and interpretation from the simulations are offered in Section 3, while a summary of the main conclusions and avenues for future work are presented in Section 4.

2. Methods

a. Experimental design

**Corresponding author address*: Brice Coffer, North Carolina State University, Campus Box 8208, Raleigh, NC, 27615-8208; *email*: becoffer@ncsu.edu

[1] These data are available from NCDC (http://www.ncdc.noaa.gov/oa/climate/severeweather/tornadoes.html#timing)

We have been exploring this problem with full-physics simulations initialized with soundings from VORTEX2. The Goshen County, WY tornadic supercell of 5 June 2009 was selected as an ideal case, due to dense temporal and spatial sounding observations through the early evening hours. The environment was characterized by a rather straight hodograph in the early afternoon, which gradually transitioned into a strongly curved hodograph in the early evening. Using a modeling technique called base-state substitution (BSS; Letkewicz et al. 2013), we are mimicking this transition in the wind profile in our simulations, without altering the thermodynamics. One advantage of BSS, is the ability to analyze how a *mature* supercell responds to increasing low-level shear, as opposed to how the supercell initially *develops*, in different background environments. Once a supercell matured in the control simulation, the original base-state (Fig. 1) wind profile was gradually modified to have stronger low-level shear (as observed), evolving through the BSS1 profile to the final BSS2 profile in Fig. 2. The only difference in the two simulations is the low-level shear. This results in noticeable differences in two common environmental forecast indices, the supercell composite parameter and significant tornado parameter, despite equal deep-layer shear, CAPE, and LCLs (Table 1).

b. Model configuration

Simulations are run using the Bryan Cloud Model 1, commonly referred to as CM1 (Bryan and Fritsch 2002). CM1 is a sophisticated moist, non-hydrostatic model well suited to idealized research of mesoscale phenomena. Using CM1 Release 16, storms were simulated in a 150 x 150 x 20 km storm-relative domain with horizontal grid-spacing of 250 m. The vertical grid was stretched from 100 m near the surface to 300 m aloft. Fine vertical resolution in the lowest couple kilometers is desirable in order to adequately resolve the low-level vorticity dynamics. Open, lateral boundary conditions and rigid, free slip upper and lower boundary conditions were used, and a Rayleigh damping sponge layer was applied above 14 km. Surface fluxes and the Coriolis force were neglected for the simplicity of isolating key processes. A relatively simple treatment of precipitation microphysics, based on Lin et al. (1983), was chosen for our initial experiments. Although any choice of parameterization will ultimately affect the four-dimensional structure of simulated convection, the general processes governing the supercell's low-level updraft are realistically represented.

3. Results

a. Convective mode

The evolution of the base reflectivity field is shown in Fig. 3. Both the Control and BSS storms maintain "classic" supercell structures through the first hour and a half after the BSS. Eventually, the outflow from the Control storm completely undercuts the updraft, leading to the demise of the control supercell and a more disorganized multicellular structure. The BSS storm remains an isolated, intense supercell.

b. Vertical vorticity profile

Time series of maximum low-level vertical vorticity for both simulations are shown in Fig. 4. The control and BSS supercells consistently produce appreciable vertical vorticity near the surface. Even though these simulations are not tornado-resolving, the BSS supercell produces a surface vortex that strengths to almost .2 s^{-1}, which is twice as strong as any produced by the Control storm. Although not shown, the vorticity throughout the storm was also enhanced, as expected due to the enhanced storm-relative helicity.

c. Updraft intensity and perturbation pressure

The BSS storm has a stronger updraft throughout the lower and middle troposphere, by roughly 10 m/s (Fig. 5). This may be due to the dynamical effects of enhanced shear or differences in the simulated cold pool temperature deficits. To look into this further, the dynamic component of the vertical perturbation pressure gradient (VPPGF) was calculated following the surface vortices. Pressure analysis was only performed while both simulations maintained supercell-like structures in the model output reflectivity field. A stronger dynamic VPPGF was observed at low-levels in the BSS storm (Fig. 6). Given that CAPE was unchanged across the experiments, it therefore appears that the dynamical effects of shear predominate the updraft differences.

This enhanced updraft would lead to greater titling and stretching of vorticity in the BSS storm.

d. Outflow ingestion

Several million parcels were released in the simulations approximately 1 hr after the BSS. These parcels were integrated forward until the Control storm no longer displayed supercellular characteristics. Outflow temperatures in both simulations were similar to one another, and not particularly cold (Fig. 7). Despite this, many more parcels entered the surface vortices in the BSS supercell. Those parcels also more frequently participated in the parent storm's updraft. The trajectories that acquired surface vorticity often stagnated in the Control storm, instead of participating in the updraft, as in the BSS storm (Fig. 8). This is indicative of a decoupling of the low-level updraft and the mesocyclone, and thus a cessation or disruption of the vortex stretching (Trapp 1999). Similar behavior is observed in nontornadic supercells. Analyzing the characteristics of the wind field in three nontornadic supercells, Markowski et al. 2011 found trajectories in the outflow rose only a few hundred meters before abruptly decelerating. They hypothesized that if the perturbation pressure-gradient force was insufficiently strong (or even adverse), then parcels will not be converged and stretched into a tornadic vortex. In our simulations, it stands to reason, that the surface vortices in the BSS supercell strengthened considerably more than the Control storm due to the stronger VPPGF at low-levels caused by the stronger low-level shear.

4. Preliminary Conclusions

Previous work has indicated a relationship between strong low-level shear and the development of intense surface vorticity in supercells. The interplay between a storm and its environment during the afternoon-evening transition is of particular interest, as this corresponds to the time of day when many tornadoes occur. Our simulations in an observed environment show that:

- As low-level shear increases, the supercell stays more organized, the profile of vertical vorticity increases in magnitude, and the updraft strengthens.
- There is evidence of both a stronger dynamic VPPGF and more outflow "participation" in the stronger-shear storm.

Future work will use more objective criteria for determining when the Control storm ceases to be a supercell. Testing the sensitivity of the simulation results to the timing and duration of the BSS is also needed, while assessing the role of dynamic and buoyant accelerations experienced by updraft parcels is currently being performed. Additionally, adding BSS of thermodynamic profiles to address the relative importance of increasing shear versus surface stabilization during the evening transition is planned. Finally, investigating another well-observed VORTEX2 case study would be beneficial for comparison.

Acknowledgements. NSF Grant AGS-1156123, George Bryan for his ongoing support of CM1, current/past members of the NCSU Convective Storms group, especially Casey Letkewicz, Adam French, and Johannes Dahl for sharing their BSS and trajectory code.

REFERENCES

Bryan, G. H., and J. M. Fritsch, 2002: A benchmark simulation for moist nonhydrostatic numerical models. *Mon. Wea. Rev*., **130**, 2917–2928.

Bonner, William D., 1968: Climatology of the Low Level Jet. *Mon. Wea. Rev.*, **96**, 833–850.

Letkewicz, C. E., A. J. French, M. D. Parker, 2013: Base-state Substitution: An Idealized Modeling Technique for Approximating Environmental Variability. *Mon. Wea. Rev.*, **141**, 3062-3086.

Lin, Y.-L., R. D. Farley, and H. D. Orville, 1983: Bulk parameterization of the snow field in a cloud model. *J. Climate Appl. Meteor.*, **22,** 1065–1089.

Maddox, R. A., 1993: Diurnal Low-Level Wind Oscillation and Storm-Relative Helicity. *The Tornado: Its Structure, Dynamics, Prediction, and Hazards, Geophys. Monogr*., **No. 79**, Amer. Geophys. Union, 591–598.

Markowski, P. M., M. Majcen, Y. P. Richardson, J. Marquis, and J. Wurman, 2011: Characteristics of the wind field in three nontornadic low-level mesocyclones observed by the Doppler On Wheels radars. *E. Journal of Severe Storms Meteor*, **6**(3), 1–48.

Markowski, P., and Y. Richardson, 2013: The influence of environmental low-level shear and cold pools on tornadogenesis: Insights from idealized simulations. *J. Atmos. Sci.*, **Accepted**.

Nieuwstadt, F. T. M. 1985: A model for the stationary, stable boundary layer. *Turbulence and diffusion in stable environments, J. C. R. Hunt, Ed., Oxford University Press*, 149-179.

Parker, M. D., 2013: Composite VORTEX2 Supercell Environments from Near-Storm Soundings. *Mon. Wea. Rev*., **Submitted**.

Trapp, R. J., 1999: Observations of nontornadic low-level mesocyclones and attendant tornadogenesis failure during VORTEX. *Mon. Wea. Rev.*, **127,** 1693–1705.

Van de Wiel, B. J. H., A. F. Moene, G. J. Steeneveld, P. Baas, F. C. Bosveld, A. A. M. Holtslag, 2010: A Conceptual View on Inertial Oscillations and Nocturnal Low-Level Jets. *J. Atmos. Sci.*, **67**, 2679–2689.

Wurman, J., D. Dowell, Y. Richardson, P. Markowski, E. Rasmussen, D. Burgess, L. Wicker, and H. B. Bluestein, 2012: The Second Verification of the Origins of Rotation in Tornadoes Experiment: VORTEX2. *Bull. Amer. Meteor. Soc.*, **93**, 1147–1170.

List of Tables and Figures

Table 1: Environmental forecast parameters for the different base-state soundings on 5 June 2009.

	6 km Shear (m/s)	3 km SRH (m2/s2)	1 km SRH (m2/s2)	1 km Shear (m/s)	CAPE (J/kg)	LCL (m)	SCP	STP
CONTROL	29.7	79	37	6.5	2837	1100	3.3	.93
BSS1	31.2	183	88	7.2	2837	1100	8.1	2.3
BSS2	30.2	401	137	12.4	2837	1100	17.2	8.1

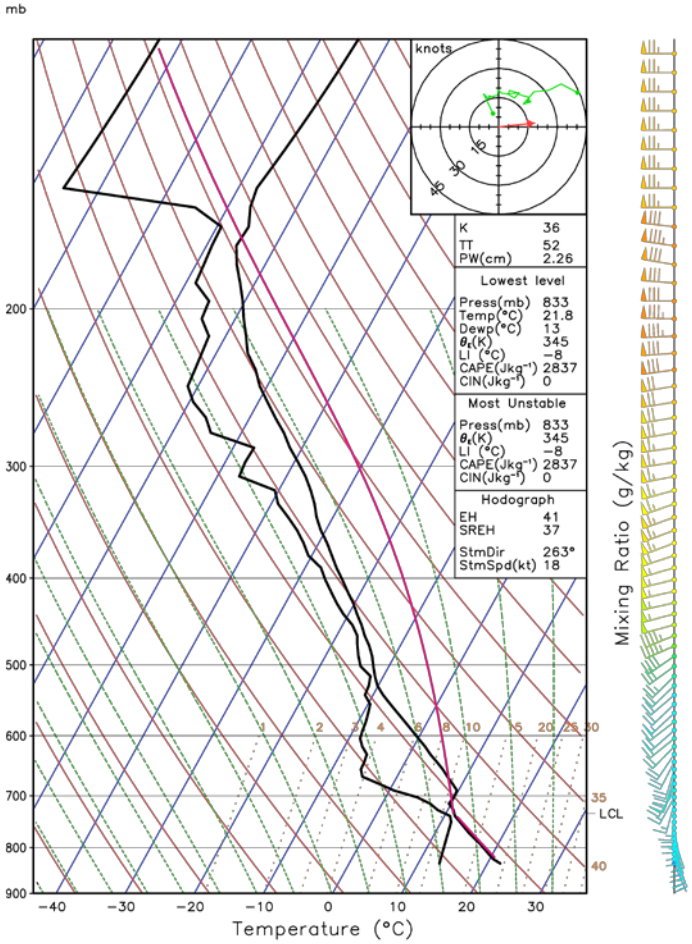

Figure 1: Sounding observed during the early afternoon of 5 June 2009.

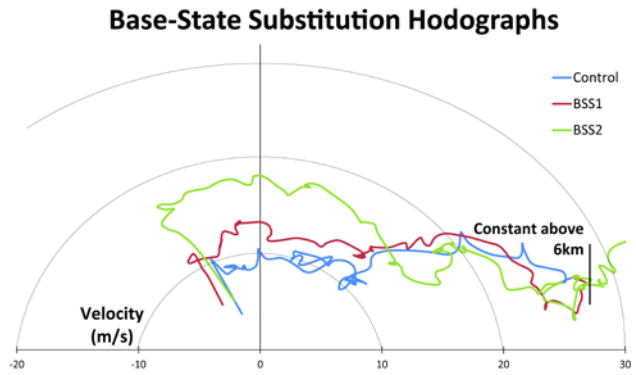

Figure 2: Hodographs for the respective base-states in Table 1.

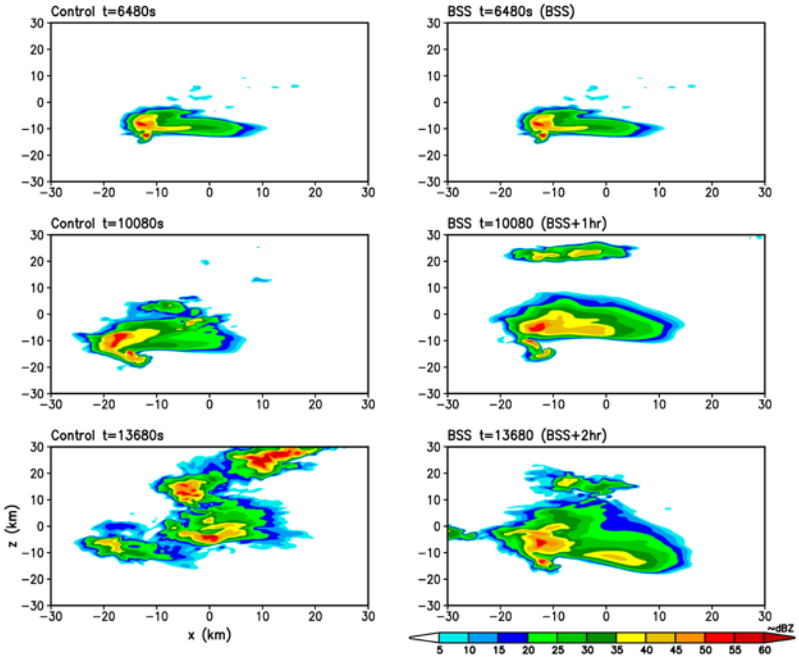

Figure 3: Model simulated base reflectivity fields for the two simulations.

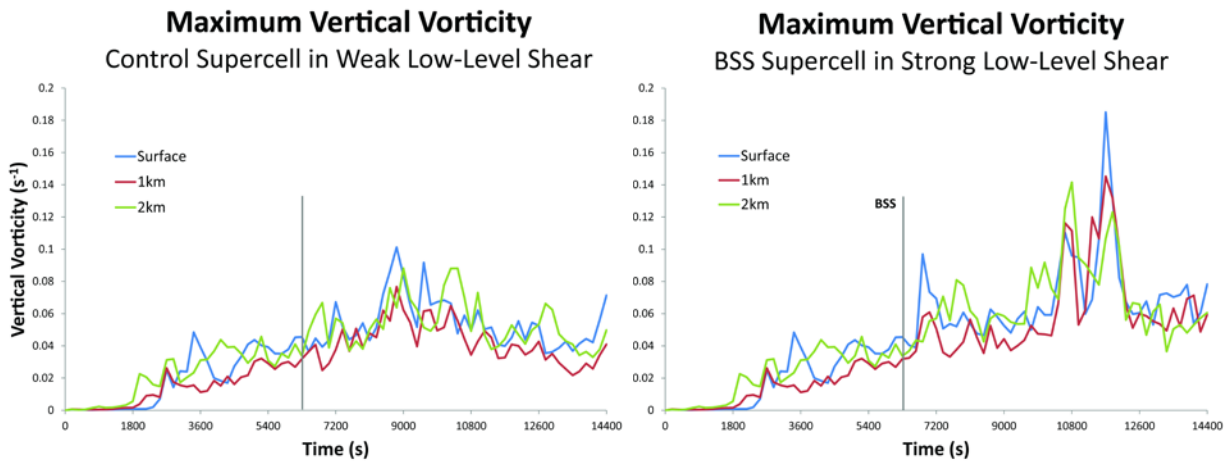

Figure 4: Time series of maximum low-level vorticity for the two simulations.

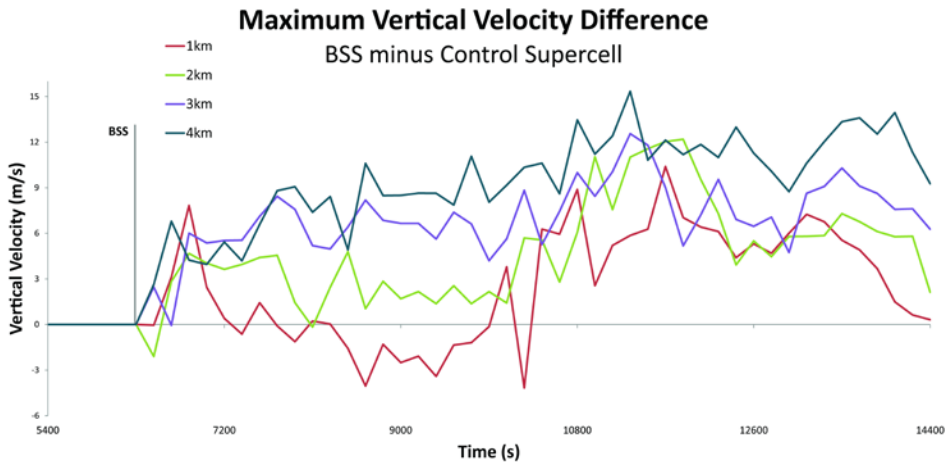

Figure 5: Time series of the difference in the maximum vertical velocity between the BSS and Control storms.

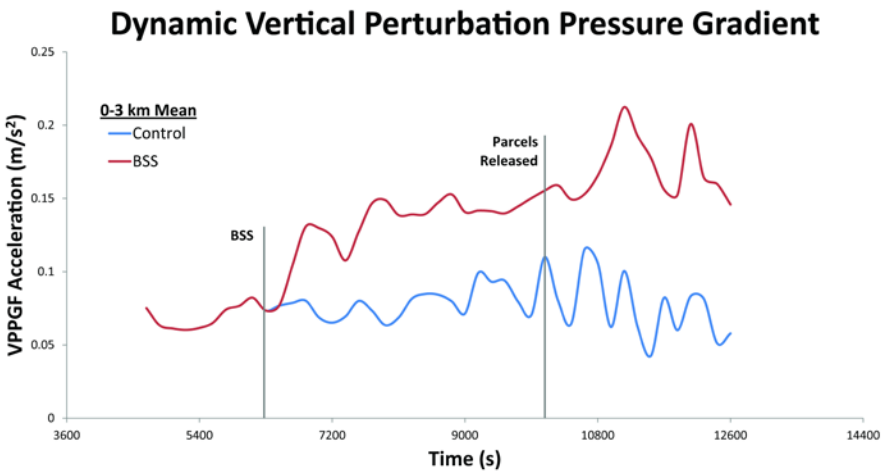

Figure 6: Time series of the 0-3 km mean dynamic vertical perturbation pressure gradient following the surface vortices.

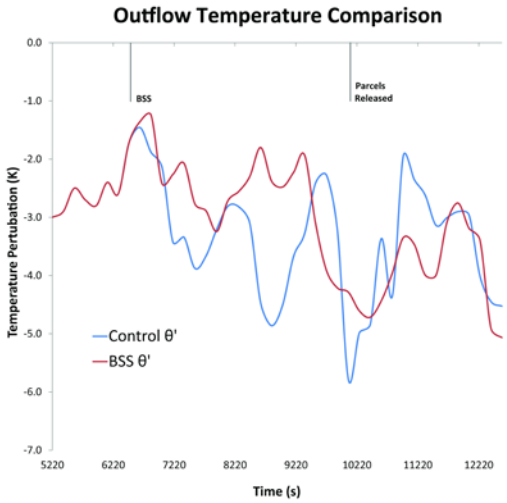

Figure 7: Time series of the mean perturbation potential temperature in the cold pool following the surface vortices.

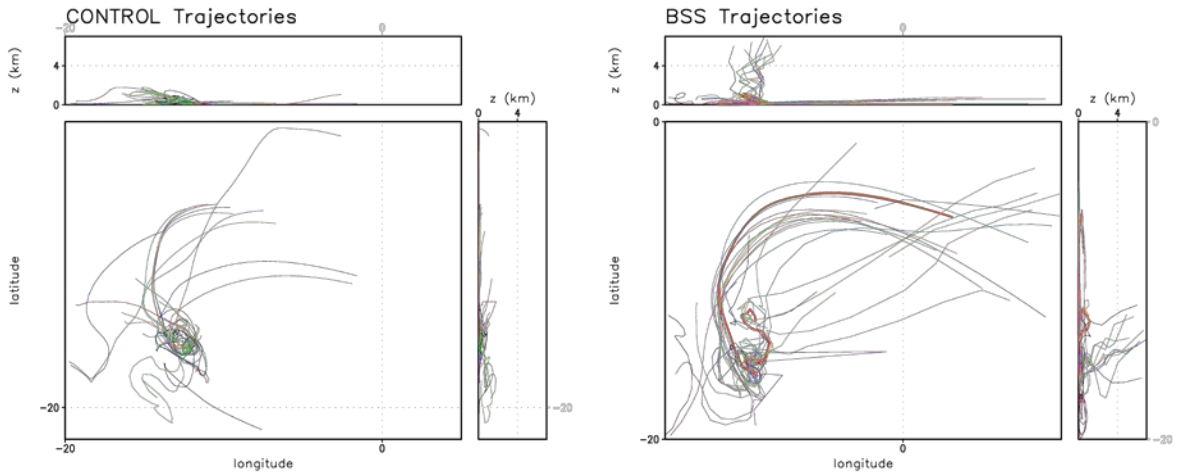

Figure 8: Trajectories of parcels that acquired appreciable surface vorticity at the lowest model level. Every 17th trajectory plotted for simplicity.